Photoresponse enhancement in the near infrared wavelength range of ultrathin amorphous silicon photosensitive devices by integration of silver nanoparticles

Etienne Moulin, Peiqing Luo, Bart Pieters, Joachim Sukmanowski, Joachim Kirchhoff, Wilfried Reetz, Thomas Müller, Reinhard Carius, Francois-Xavier Royer, and Helmut Stiebig

Articles you may be interested in

Photoresponse enhancement in the near infrared wavelength range of ultrathin amorphous silicon photosensitive devices by integration of silver nanoparticles

Etienne Moulin,[1,a] Peiqing Luo,[1] Bart Pieters,[1] Joachim Sukmanowski,[2] Joachim Kirchhoff,[1] Wilfried Reetz,[1] Thomas Müller,[1] Reinhard Carius,[1] Francois-Xavier Royer,[3] and Helmut Stiebig[4]

[1]*IEF5 Photovoltaik, Forschungszentrum Jülich, 52425 Jülich, Germany*
[2]*Institute of Experimental Physics, Saarland University, Postfach 151150, D-66041 Saarbruecken, Germany*
[3]*Laboratoire de Physique des Milieux Denses (LPMD), Université de Metz, 1 Bd Dominique François ARAGO, F-57078 Metz, France*
[4]*Malibu GmbH & Co. KG, Boettcherstrasse 7, D-33609 Bielefeld, Germany*

We have investigated the contribution of localized surface plasmon polaritons (LSPPs) in silver nanoparticles with radii smaller than 20 nm to the photocurrent of ultrathin photosensitive devices based on amorphous silicon. An increased light absorption and an enhanced photocurrent are found for wavelengths between 600 nm and 1150 nm in presence of nanoparticles. As amorphous silicon absorbs light efficiently only at wavelengths up to 750 nm, the increased photocurrent in the near infrared range is explained in terms of LSPP-induced photoemission of electrons within and in close vicinity of the nanoparticles. © *2009 American Institute of Physics*. [DOI: 10.1063/1.3157264]

Metal nanoparticles (NPs) show resonances in their absorption and scattering spectra, denoted as localized surface plasmon polariton (LSPP) resonances, which are a consequence of the collective oscillation of the free electrons of the metal NP.[1,2] Several authors have made use of the light scattering (amplified at the LSPP resonances) of large metal NPs (with radii R between 25 and 150 nm) to improve the light absorption of crystalline and amorphous silicon (a-Si:H) solar cells.[3–6] The optical response of small metal NPs ($R < 20$ nm) is characterized by a single LSPP resonance [dipolar surface plasmon polariton resonance]. Under these conditions the LSPP resonance is accompanied by a strong enhancement of the electromagnetic field inside and in close vicinity of the NPs.[1,2] Enhanced photovoltaic conversion efficiencies of organic and dye-sensitized thin-film solar cells containing small metal NPs have already been demonstrated.[7–9] The observed increase in photocurrent is explained in terms of (i) improved light absorption in the active layer of the cell, due to the enhanced electromagnetic field in the vicinity of the NPs at the LSPP resonance or (ii) photoexcitation of electrons from the NPs to their surrounding. The positive contribution of surface plasmon polaritons (SPPs) on the photocurrent of inorganic semiconductor/metal Schottky junctions has also been reported by using the method of attenuated total reflection.[10] Under these conditions, the enhanced photocurrent is explained in terms of photoexcitation of electrons from the metal surface to the semiconductor at the SPP resonance.

In order to investigate the local contribution of small metal NPs for thin-film silicon solar cell applications, Ag NPs of various sizes ($R < 20$ nm) were deposited at the transparent conductive oxide (TCO)-i interface of ultrathin a-Si:H photosensitive devices in the Ag/TCO/i/p/TCO and Ag/TCO/i/n/TCO configurations [see Fig. 1(a)]. Under these conditions, the NPs are in direct contact with the active

layer (the i-layer) of the device. The NPs were prepared by thermal evaporation of a thin Ag film at a pressure of approximately 10^{-5} mbar and a postannealing treatment in vacuum at a temperature of 180 °C for 90 min. In order to obtain NPs of various sizes the thickness of the Ag film was varied between 2 and 5 nm. The Ag bulk layer of the glass/Ag/TCO back reflector and the 80 nm thick back- and front-TCO films were deposited by sputtering at room temperature. The 20 nm thick a-Si:H i-, n-, and p-layers were deposited by plasma enhanced chemical vapor deposition.

Figure 1(b) shows a SEM (scanning electron microscope) picture of a 2 nm Ag film on glass/Ag/TCO after annealing treatment at 180 °C for 90 min. Well separated NPs with a broad distribution of sizes and an average radius of 10 nm are obtained. By increasing the thickness of the Ag film, the average radius of the NPs increases. For 5 nm Ag, NPs with an average radius of around 20 nm are formed after annealing (not shown). The influence of the NPs on the re-
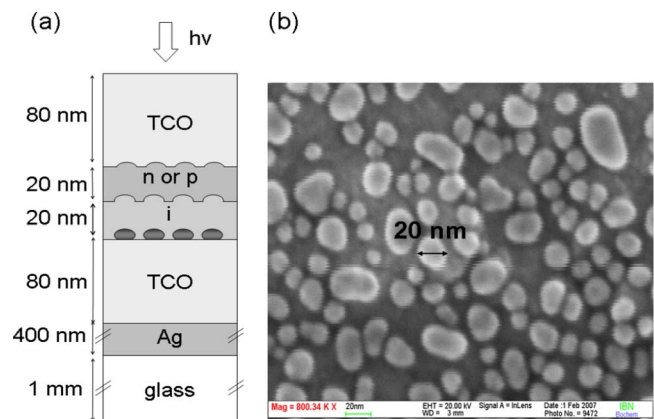

FIG. 1. (Color online) (a) Schematic drawing of the investigated a-Si:H devices in the Ag/TCO/i/n/TCO or Ag/TCO/i/p/TCO configuration. The NPs are positioned at the TCO/i interface. (b) SEM picture of a 2 nm Ag film on glass/Ag/TCO after annealing treatment at 180 °C for 90 min.
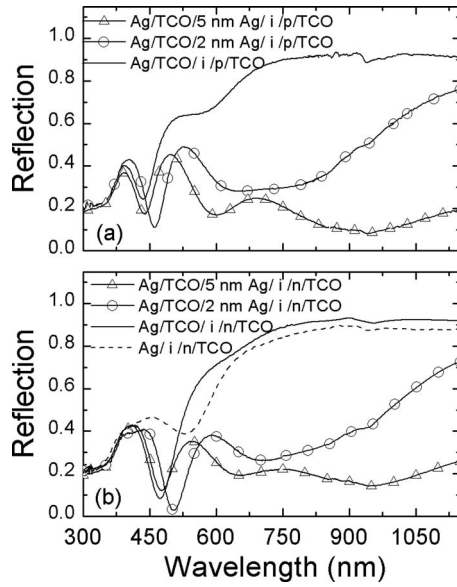
[a]Electronic mail: e.moulin@fz-juelich.de.

FIG. 2. Reflection measurements of (a) Ag/TCO/(NPs)/i/p/TCO and (b) Ag/TCO/(NPs)/i/n/TCO devices with and without nanoparticles resulting from the thermal evaporation of 2 and 5 nm Ag films.

flectivity of the Ag/TCO/i/p/TCO and Ag/TCO/i/n/TCO devices is shown in Figs. 2(a) and 2(b), respectively. Independent of the device configuration, the layer stacks with Ag NPs show a strong decrease in the reflectivity for wavelengths λ larger than 500 nm in comparison to the layer stacks without NPs, which is ascribed to LSPP absorption of the NPs. For thicker evaporated Ag films, the minimum in reflectivity becomes broader and is redshifted due to the larger sizes of the obtained NPs.[11,12] We assume that the broad minimum in the reflectivity is due to (i) the presence of the Ag back reflector, which leads to interferences that partly mask the LSPP resonance and (ii) a broadening of the LSPP resonance originating from the large distribution in shapes and sizes of the NPs.

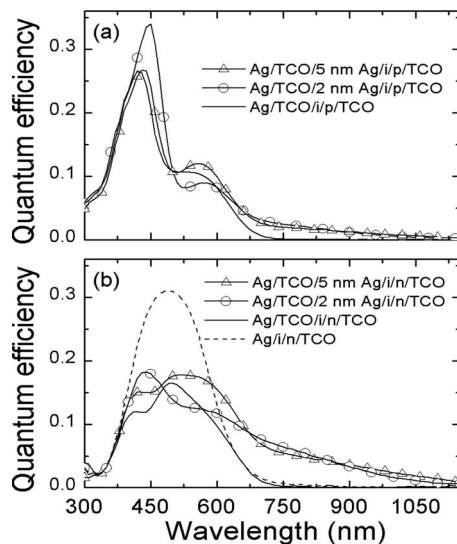Figures 3(a) and 3(b) show the quantum efficiency (QE) at 0 V of devices in the Ag/TCO/(NP)i/p/TCO and

FIG. 3. QE of (a) Ag/TCO/(NPs)/i/p/TCO and (b) Ag/TCO/(NPs)/i/n/TCO devices with and without NPs resulting from the thermal evaporation of 2 and 5 nm Ag films. For comparison, the QE of the bulk-Ag/i/n/TCO device is also shown.
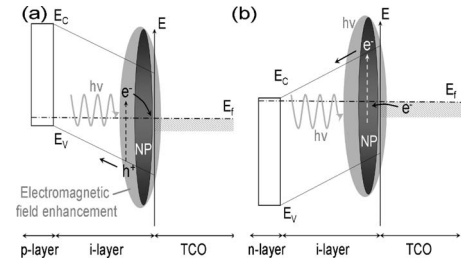

FIG. 4. Illustration of possible photoemission processes occurring in the (a) Ag/TCO/(NPs)/i/p/TCO and (b) Ag/TCO/(NPs)/i/n/TCO devices. Photoexcitation from states inside and in the vicinity of the NP at the LSPP resonance, charge separation, and transport processes are depicted. The symbols e^- and h^+ represent electrons and holes, respectively.

Ag/TCO/(NPs)i/n/TCO configuration, respectively. In the short wavelength range, the QE of the devices with and without NPs is nearly identical. For λ > 600 nm, the photosensitive devices containing NP show an enhanced photocurrent compared to the devices without NPs. For λ > 750 nm no photocurrent is measured for the devices without NPs. In this wavelength range, a-Si:H does not absorb light efficiently, due to its band gap of around 1.7 eV. However, a photocurrent is measured in the near infrared range (NIR) for devices with NP. The broad enhancement of the photocurrent correlates with the broad reflectivity minimum found in presence of NPs. By increasing the Ag film thickness from 2 to 5 nm, and consequently the average size of the resulting NPs, the contribution of the photocurrent slightly shifts to longer wavelengths. Raman measurements of devices containing Ag NPs show a broadband centered at 480 cm^{-1}, which is characteristic of a-Si:H (not shown). However no Raman peak at 520 cm^{-1}, characteristic of microcrystalline silicon, is found in the Raman spectrum. Therefore, we conclude that the Ag NPs does not induce the crystallization of the a-Si:H. Thus, the gain in the photocurrent observed for λ > 750 nm cannot be explained by an improved light absorption due to an alteration of the a-Si:H. We have carefully checked whether the enhanced photocurrent is due to a temperature effect resulting from enhanced light absorption in the NPs at the LSPP resonance. The photocurrent of the device without NPs increases by enhancing the device temperature. However even at 100 °C the photocurrent of the device without NPs remains much lower than the photocurrent of the device with NPs measured at room temperature. The temperature of the device is required to be far above 100 °C in order to account for the measured photocurrent. We proved that the open circuit voltage was almost identical for 532 and 897 nm when the same generation rate (short circuit current) was used. It is therefore concluded that the mechanism at these two wavelengths is the same and that a photovoltaic effect and no other effect such as thermopower is involved. Since a-Si:H absorbs light efficiently only at wavelengths up to 750 nm, the measured photocurrent in the NIR can also not be explained by an enhanced light absorption in the bulk a-Si:H i-layer. Photoexcitation of electrons within or in the vicinity of the NPs may explain the increased QE in the NIR. Figures 4(a) and 4(b) show schematic models of possible photoemission processes involved in the carrier-generation mechanism for the Ag/TCO/NPs/i/p/TCO and Ag/TCO/NPs/i/n/TCO structures, respectively. The TCO/NP/i layer stack forms a Schottky contact. In case of the Ag/TCO/NPs/i/p/TCO structure, electrons can be gen-

erated by photoexcitation from the valence band of the *i*-layer into the TCO/NP contact. The *p*-type contact allows extraction of holes from the *i*-layer leading to a photocurrent. For the Ag/TCO/NPs/*i*/*n*/TCO, an electron can be generated by photoexcitation from the TCO/NP contact into the conduction band of the *i*-layer. The *n*-type contact allows extraction of electrons. For both structures, the photoexcitation of electrons can be enhanced by the LSPP-induced increase in the electromagnetic field within and in the surrounding of the NP. The Ag/TCO/NPs/*i*/*n*/TCO structure clearly shows a larger enhancement of photocurrent in the NIR than the Ag/TCO/NPs/*i*/*p*/TCO structure. This difference may be explained by a difference in probability between excitation of electrons within the NP and excitation of electrons in the *i*-layer in close vicinity of the NP.

In order to verify that the photocurrent enhancement is actually caused by the LSPP effect in the NPs, a bulk-Ag/*i*/*n*/TCO layer stack was prepared. The Ag bulk layer consists of a 700 nm Ag film deposited by thermal evaporation. Reflection measurements of the bulk-Ag/*i*/*n*/TCO layer stack show a slight decrease in the reflectivity in the long wavelength range [Fig. 2(b), dashed line] compared to the Ag/TCO/*i*/*n*/TCO layer stack, probably due to absorption losses in the bulk Ag.[13] The QE of the prepared layer stack exhibits a high signal in the short wavelength range due to interferences. However, no photocurrent is measured for $\lambda > 750$ nm, as shown in Fig. 3(b) (dashed line). Thus, we conclude that the enhanced photocurrent in the NIR observed in the case of devices containing Ag NPs is caused by the resonant LSPP effect of the NPs.

In summary Ag NPs with radii below 20 nm were deposited by thermal evaporation and postannealing treatment at the TCO-*i* interface of ultrathin *a*-Si:H devices in the Ag/TCO/*i*/*n*/TCO and Ag/TCO/*i*/*p*/TCO configurations. Independently of the device configuration, an enhanced light absorption is observed in the long wavelength range for devices with NPs compared to devices without NPs, attributed to LSPP. The devices containing Ag NPs show an enhanced photocurrent in the NIR region of the spectrum. Since *a*-Si:H only efficiently absorbs light for wavelengths up to 750 nm, we assume that photoexcitation of electrons from the NPs or from states in close vicinity of the NPs at the LSPP resonance is responsible for the increased photocurrent. Theoretical investigations have to be made to verify the validity of the suggested explanation.

[1] U. Kreibig and M. Vollmer, *Optical Properties of Metal Clusters* (Springer, Berlin, 1995).

[2] S. A. Maier, *Plasmonics: Fundamentals and Applications* (Springer, New York, 2007).

[3] D. Derkacs, S. H. Lim, P. Matheu, W. Mar, and E. T. Yu, Appl. Phys. Lett. **89**, 093103 (2006).

[4] D. M. Schaadt, B. Feng, and E. T. Yu, Appl. Phys. Lett. **86**, 063106 (2005).

[5] S. Pillai, K. R. Catchpole, T. Trupke, and M. A. Green, J. Appl. Phys. **101**, 093105 (2007).

[6] E. Moulin, J. Sukmanowski, P. Luo, R. Carius, F. X. Royer, and H. Stiebig, J. Non-Cryst. Solids **354**, 2488 (2008).

[7] M. Westphalen, U. Kreibig, J. Rostalski, H. Lüth, and D. Meissner, Sol. Energy Mater. Sol. Cells **61**, 97 (2000).

[8] O. Stenzel, A. Stendal, K. Voigtsberger, and C. von Borczyskowski, Sol. Energy Mater. Sol. Cells **37**, 337 (1995).

[9] C. Wen, K. Ishikawa, M. Kishima, and K. Yamada, Sol. Energy Mater. Sol. Cells **61**, 339 (2000).

[10] C. Daboo, M. J. Baird, H. P. Hughes, N. Apsley, and T. Emeny, Thin Solid Films **201**, 9 (1991).

[11] C. Sönnichsen, T. Franzl, T. Wilk, G. von Plessen, J. Feldmann, New J. Phys. **4**, 93 (2002).

[12] C. Sönnichsen, S. Geier, N. E. Hecker, G. von Plessen, J. Feldmann, H. Ditlbacher, B. Lamprecht, J. R. Krenn, F. R. Aussenegg, V. Z.-H. Chan, J. P. Spatz, and M. Moeller, Appl. Phys. Lett. **77**, 2949 (2000).

[13] J. Springer, A. Poruba, L. Müllerova, M. Vanecek, O. Kluth, and B. Rech, J. Appl. Phys. **95**, 1427 (2004).